15th Canadian Masonry Symposium
Ottawa, Canada
June 2-5, 2025

Finite Element Micro-Modelling of North American Partially Grouted Masonry Shear Walls

Dina Helmy[i], Carlos Cruz-Noguez[ii], and Clayton Pettit [iii]

ABSTRACT

Partially-grouted concrete block masonry walls are an attractive gravity and lateral load resisting system due to their low seismic mass, thermal efficiency, and constructability. Contrary to fully-grouted walls where all cells within the masonry wall are filled with grout, partially-grouted walls only feature grout in cells containing steel reinforcement. While resulting in a more economical solution compared to fully-grouted walls, the presence of voids in partially grouted walls creates difficulties in analyzing the wall system using conventional mechanics-based methods. This, compounded with the complexities associated with the block-mortar and block-grout interfaces, has resulted in a noticeable lack of understanding towards the behaviour of partially-grouted walls under in-plane lateral loads. In this study, a finite element (FE) methodology for micro-modelling partially-grouted concrete block masonry walls subjected to in-plane loading is developed. Within the FE framework, all cementitious components (masonry units, mortar, and grout) are separately modeled as two-dimensional solid continuum elements while reinforcing bars as beam elements. Interfaces existing between the masonry units, mortar, and grout are accounted for and defined through contact-based cohesion models. Several experimental studies were selected to validate the model and ensure the robustness of the modelling methodology under different loading scenarios and wall configurations. Examples of parameters investigated include wall openings, incorporation of bond beam and/or bed-joint reinforcement, cyclic loading, and wall aspect ratio. Results of the micro-model simulation for each experimental study are presented and followed by a detailed discussion of the performance, limitations, and applications of the micro-model.

KEYWORDS

Masonry, Shear Walls, Partially-Grouted, Finite Element, Micro-Modelling

[i] Ph.D. Student, University of Alberta, Edmonton, Canada, dhelmy@ualberta.ca. Corresponding Author.
[ii] Professor, University of Alberta, Edmonton, Canada, cruznogu@ualberta.ca.
[iii] Assistant Professor, University of Alberta, Edmonton, Canada, cpettit@ualberta.ca.

INTRODUCTION

Masonry walls are widely used in building construction globally due to their durability and versatility. While historical masonry walls were typically unreinforced, modern designs incorporate reinforcement to enhance their strength and ductility. Reinforced masonry walls are categorized as fully grouted, where all cells are filled with high-slump grout, or partially grouted, where only cells containing reinforcement are grouted. The latter has gained popularity in low- to mid-seismic regions due to its economic benefits, ease of construction, and lower seismic mass. However, designing partially grouted walls to resist in-plane shear remains challenging due to the complex interaction among their components and the varied failure mechanisms they exhibit.

Early investigations into the in-plane shear behaviour of reinforced masonry walls began in the mid-1970s [1][2][3][4] with studies on fully grouted masonry piers of different aspect ratios. These studies formed the foundation for the first in-plane shear strength equation, introduced in the 1994 National Earthquake Hazards Reduction Program (NEHRP) [5] design provisions. This equation, later adopted by Canadian and American design standards such as CSA S304 [6] and TMS 402/602 [7], has remained relatively unchanged for over three decades. Despite advancements in construction techniques and material science, recent studies have shown that these equations often yield inconsistent predictions, with some unconservative results, raising concerns about their reliability given the brittle nature of shear failure. Experimental testing, though effective, is resource-intensive, prompting researchers to explore computational approaches as a cost-efficient alternative.

Three primary modelling approaches have emerged for masonry walls: macro-modelling, simplified micro-modelling, and detailed micro-modelling. Macro-modelling treats the wall as a single homogeneous entity, ignoring interactions between components and limiting its ability to capture localized phenomena such as step-cracking [8][9]. Simplified micro-models address these limitations by introducing interface characteristics between masonry units. However, these models often lack the resolution needed to capture stress concentrations and localized failures, such as grout crushing, and are primarily suited for unreinforced walls [10][11][12]. Detailed micro-models explicitly represent each masonry component and their interfaces, offering superior accuracy in simulating behaviour [13][14]. However, the high computational demand of these models has limited their use to a few studies, particularly for reinforced systems.

Recent research has developed specialized micro-models for partially grouted walls, successfully capturing both global and local responses, including load-displacement behaviour, failure modes, and cracking patterns. Despite these advancements, existing studies have primarily focused on monotonic loading conditions and specific masonry configurations, such as multi-perforated clay brick walls with bed joint reinforcement. These limitations make it challenging to generalize the findings to typical North American masonry walls featuring concrete blocks and bond beams, especially under cyclic loading scenarios observed in seismic events.

This study seeks to address these gaps by developing and validating a generalized finite element micro-modelling methodology for partially grouted masonry walls, accommodating various materials such as clay bricks and concrete blocks. The proposed methodology aims to accurately represent the detailed geometry and interactions among components while capturing localized phenomena such as grout crushing, block cracking, and interface separation. By focusing on these aspects, the study strives to predict the in-plane behaviour of partially grouted masonry walls and enhance the understanding of stress distributions and failure mechanisms, providing a robust foundation for future design practices.

FINITE ELEMENT MICRO-MODEL DEVELOPMENT

The detailed micro-model was developed to incorporate the non-prismatic characteristics of masonry wall systems while maintaining computational efficiency by restricting the model to two dimensions. This approach balances accuracy with practicality, enabling detailed analysis without excessive computational demands. The model was implemented using the finite element software ABAQUS (Dassault Systems, 2022)[15], which provided the necessary tools for precise geometry and material representation.

The wall geometry was divided into two distinct layers of uniform thickness to reflect the structural components accurately, see Fig. 1a. The first layer, referred to as the "masonry layer," represents the masonry unit flanges stacked between segments of mortar, as illustrated in Fig. 1b. The second layer, termed the "grout layer," includes the masonry unit webs, grout cores, vertical reinforcement, and horizontal reinforcement, as shown in Fig. 1c. This layered representation ensures that the complex interactions between different components of the wall system are adequately captured.

Quadratic quadrilateral continuum elements with full integration were used to model the masonry units, mortar, grout cores, foundations, and capping beam. A fine mesh density with an element size of 20 mm was employed to achieve detailed stress and strain predictions across these components. For the reinforcement, linear beam elements were specified to represent both vertical and horizontal steel accurately. This modelling framework combines a refined geometric representation with efficient computational techniques, making it well-suited for analyzing the behaviour of masonry wall systems under various loading conditions.

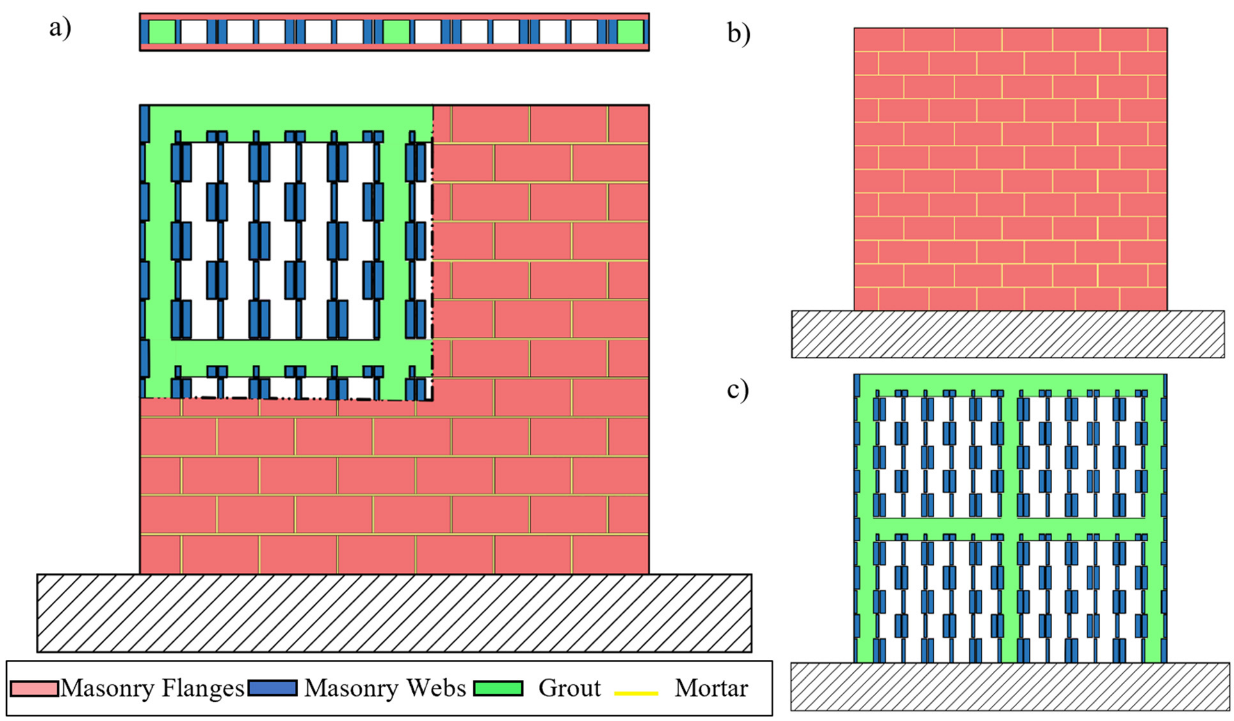

Figure 1: Micro-model layers a) A section in the wall revealing the different layers, b) Masonry layer, b) Grout layer.

To couple the masonry layer with the grout layer, embedment constraints were implemented. This constraint type ensures that the translational degrees of freedom of an embedded set of elements (masonry web elements) are constrained to those of the host region elements (masonry flange elements). As a result, the embedded elements maintain their relative position with respect to the host elements during loading, enabling accurate load transfer and interaction between the components.

Within the two-layer system, the embedment constraints were specifically defined for two purposes: (1) to embed both the horizontal and vertical reinforcement bars within the solid grout elements and (2) to embed the masonry unit web elements within the masonry unit flanges. This configuration facilitates the transfer of mechanical loading applied to the grout core through a series of defined contact interfaces. The load is first transferred to the masonry webs via the contact between the grout cores and masonry webs and subsequently transferred from the masonry webs to the masonry flanges through the embedment constraints.

To accurately capture the interaction between the components, contact interfaces were defined at critical regions, including those between the grout cores and masonry webs and between the masonry flanges and mortar layers. These interfaces were modeled using a combination of a Mohr-Coulomb friction law and a surface-based cohesion model. The combined model is governed by a linear traction-separation law, which accounts for the stiffness of the cohesive interface and incorporates a damage criterion based on the applied normal and shear stress ratios to their respective maximum limits. Upon reaching the damage limit state, the cohesive properties of the interface degrade exponentially, and the interface behaviour transitions to being solely governed by the Mohr-Coulomb friction law. This approach ensures a realistic representation of load transfer and interface behaviour, capturing the progressive deterioration and ultimate failure of the masonry system under loading.

MATERIAL MODELS

Two material plasticity models were employed in the finite element model to represent the behaviour of steel reinforcement and masonry materials. The first model, a uniaxial plasticity model, was used to capture the elastic and strain-hardening behaviour of the steel reinforcement. The second model, the history-dependent Concrete Damage Plasticity (CDP) model [16][17], was utilized to simulate the nonlinear response of the masonry units, mortar, and grout. The CDP model defines the biaxial response of cementitious materials based on a uniaxial stress-strain relationship for both tensile and compressive behaviours, making it well-suited for capturing the complex behaviour of masonry systems.

The CDP model requires the specification of five additional field parameters to fully define the material behaviour. These parameters include the dilation angle, eccentricity, the ratio of biaxial compressive yield stress to uniaxial yield stress, the ratio of the second stress invariant on the tensile mean, and the viscosity parameter. The dilation angle and eccentricity account for the dilatancy observed in cementitious materials, where volumetric strain increases under shear deformation. This phenomenon necessitates the use of a non-associated flow rule, rather than an associated flow rule, within the CDP model. The Drucker-Prager hyperbolic function is used to model the effective stress envelope in the normal stress–shear stress (p-q) plane, where the dilation angle defines the slope of the linear relationship, and the eccentricity smooths the hyperbolic function as shear stress approaches zero. Values of 30° and 0.1 were assigned to the dilation angle and eccentricity, respectively, based on recommendations from previous research [18][19][20][21][22][23].

Additional parameters were specified based on established practices for concrete materials. The ratio of biaxial compressive yield stress to uniaxial yield stress was set at 1.16, while the ratio of the second stress invariant on the tensile mean was taken as 2/3, both of which are default values widely accepted for concrete-like materials. The viscosity parameter, crucial for the visco-plastic regularization employed in the model, was set to 0.0002. This value was determined through iterative simulations in which the parameter was incrementally increased until a significant change in the load-displacement response of the wall was observed. Higher viscosity values were found to reduce computational runtime but at the expense of accuracy. It is important to note that due to the visco-plastic regularization, the model response exhibited some dependency on the size of the pseudo-timestep, even during static analyses. These considerations highlight the careful calibration required to balance accuracy and computational efficiency in modelling masonry systems.

The uniaxial compressive behaviour of all masonry materials in the model was characterized using the Hognestad parabola [24], as illustrated in Fig. 2a. This model was selected for its versatility, allowing the complete uniaxial compressive stress-strain response of a material to be defined using only two parameters: the peak compressive stress and either the corresponding strain at peak stress or the material's initial elastic modulus. While peak compressive stress values for masonry units, mortar, and grout are commonly reported in the literature, data on their elastic modulus and peak strain are less frequently available. To address this, the elastic modulus of the masonry unit, mortar, and grout was estimated using research focused on the behaviour of concrete masonry assemblages [25], the Canadian concrete design provisions (CSA A23.3-19), and the American masonry design provisions (TMS 402/602-16), respectively.

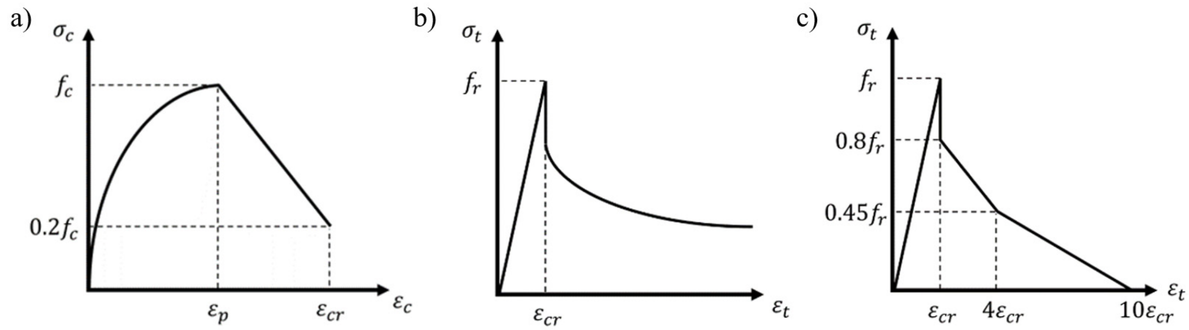

Figure 2: Uniaxial Response (a) Masonry, Mortar, and Grout in Compression (b) Grout in Tension (c) Masonry and Mortar in Tension

For post-peak compressive behaviour, the stress-strain model proposed by Priestley and Elder [26], a modified version of the Kent and Park [27] model for concrete, was employed for all masonry materials. Unlike the Hognestad model, which assumes a quadratic softening response, the Priestley and Elder model assumes a linear softening profile, providing a more realistic representation of post-peak behaviour.

The tensile response of the grout was modeled using the tensile model proposed by Vecchio and Collins [28], which assumes linear elastic behaviour until rupture, followed by tension softening, as shown in Fig. 2b. Conversely, the tensile response of the masonry units and mortar was represented by the model proposed by Nayal and Rasheed [29], depicted in Fig. 2c. The primary distinction between these models lies in the rate of tensile degradation. The Vecchio and Collins [28] model features a slower degradation rate due to its assumption of steel reinforcement within the material, a condition that is valid for the grout cores but not applicable to the masonry units and mortar. This differentiation in tensile modelling ensures that the behaviour of each material component is accurately captured within the micro-model. These models collectively provide a robust framework for representing both compressive and tensile behavior across the masonry system, enabling accurate simulation of the mechanical responses under various loading conditions.

The final parameters defined in the Concrete Damage Plasticity (CDP) model are two scalar damage parameters and two stiffness recovery factors, which account for the degradation of stiffness in cementitious materials under cyclic loading. The scalar damage parameters (d_c for compression and d_t for tension) are widely used in damage-based models for concrete [30][31] and represent the reduction in stiffness due to material degradation. These parameters are applied by reducing the elastic modulus of the material by a factor of d_c and d_t in compression and tension, respectively. Their implementation is similar to that of the uniaxial true stress-plastic strain curve, where specific values of the damage parameters are defined for different regions of inelastic strain. The compressive and tensile damage parameters used in the model were calculated based on the expressions proposed by Obaidat [32] and Birtel and Mark [33], respectively.

In addition to the damage parameters, two stiffness recovery factors (w_c for compression and w_t for tension) were included in the model. These factors control the extent to which stiffness is regained when the material transitions between compression and tension loading states. The recovery factors are essential for accurately modelling the cyclic behaviour of cementitious materials, as they allow for partial stiffness recovery during load reversals, which is critical for realistic simulations of cyclic loading conditions.

Figure 3 illustrates the cyclic behaviour of the CDP model, highlighting the role of the damage parameters and stiffness recovery factors. The inclusion of these parameters enhances the ability of the model to simulate the degradation and recovery of stiffness under cyclic loading, providing a more comprehensive representation of the mechanical behaviour of masonry systems. This approach ensures that the model can accurately capture the progressive damage and recovery processes observed in cementitious materials subjected to complex loading conditions.

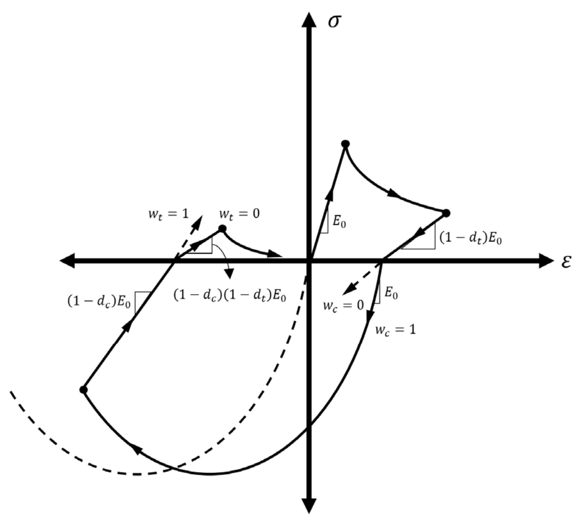

Figure 3: Cyclic Response of the Concrete Damage Plasticity Model.

FINITE ELEMENT MICRO-MODEL VALIDATION

The micro-model was validated using the experimental study conducted by Nolph and ElGawady [34], which included a total of 4 walls subjected to combined axial and lateral loading. These walls featured variations in key parameters, such as aspect ratio, vertical reinforcement quantity and spacing, horizontal reinforcement quantity, and reinforcement type (bond beam vs. bed-joint reinforcement). The geometry and reinforcement distribution of the walls are illustrated in Fig. 4, while the material properties and reinforcement quantities specified for the micro-model are presented in Table 1. Since the peak compressive strength of the mortar was not explicitly provided by Nolph [35], the value from a related study conducted by Elmapruk [36] was adopted, as the two studies were carried out in conjunction.

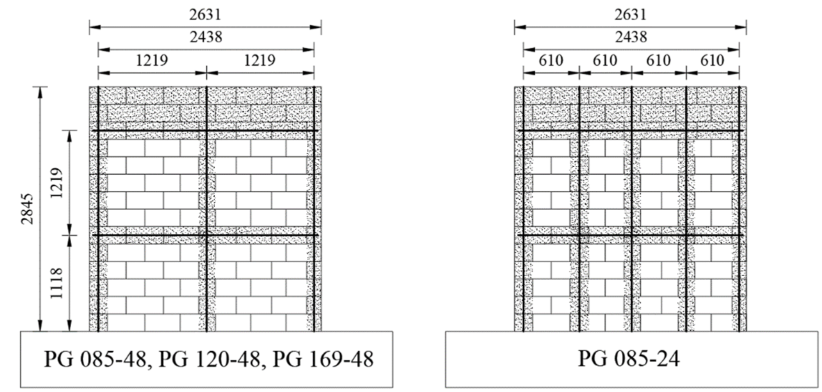

Figure 4: Wall Geometry of Tested Specimens from Nolph and ElGawady [34]

Table 1. Reinforcement Quantities and Material Properties from Nolph and ElGawady [34]

Study	**Specimen**	**Axial Load Level (MPa)**	**Reinforcement Ratio (%)**		**Compressive Strength (MPa)**			**Yield Strength (MPa)**	
			Horizontal	Vertical	Masonry/ Brick	Mortar	Grout	Horizontal	Vertical
Nolph	PG085-24	0.10	0.085	0.500	18.1	14.9	29.2	439	439
	PG085-48	0.10	0.085						
	PG120-48	0.10	0.120						
	PG169-48	0.10	0.169						

To evaluate the cyclic performance of the micro-model, an additional cyclic simulation was performed for Specimen PG085-48 from the Nolph and ElGawady [34] study. This specimen was selected as it features the most representative design parameters for partially grouted masonry walls. All walls in the study were tested in a cantilever configuration, with a fixed base boundary condition applied by restraining the base of the concrete foundation from translating in both horizontal and lateral directions.

For loading, a two-step static analysis was used. In the first step, an axial stress of 0.1 MPa was applied to the top of the model and maintained throughout the second step, during which a lateral displacement was specified at multiple nodes along the top of the wall. These nodes were spaced approximately 400 mm apart to correspond to the placement of the steel bolts used to secure the steel loading beam to the top of the wall system. The vertical degrees of freedom of these nodes were left unconstrained to allow rotation along the top of the wall, accurately simulating cantilever boundary conditions. All walls were constructed using standard (8-inch) hollow masonry units in a running bond pattern, reflecting common construction practices and ensuring the model's validity under realistic loading scenarios.

Figure 5 presents a comparison of the load–drift response obtained from the finite element micro-model and experimental testing for four specimens. The micro-model demonstrated strong agreement with the experimental data in predicting the ultimate load capacity, with predictions deviating between 5% and 14% of the experimentally observed values. This highlights the model's accuracy in capturing the peak load-bearing capacity of the masonry walls under combined axial and lateral loading.

In terms of stiffness, the micro-model exhibited a tendency to over-predict the stiffness after the initial loading cycles. This discrepancy is attributed to the absence of damage models in the representation of both the reinforcing steel and cohesive interfaces. These limitations result in a less accurate depiction of the progressive degradation of stiffness that occurs during cyclic loading.

Despite these limitations, the overall behaviour predicted by the micro-model closely aligned with the experimentally observed behaviour. The model effectively replicated the diagonal tension failure mode reported in the experiments, characterized by prominent diagonal crack openings followed by compression toe crushing. Additionally, the model was consistent with experimental findings in that no significant yielding of the horizontal reinforcement was observed for the majority of specimens. These results underscore the effectiveness of the micro-model in capturing critical failure mechanisms and overall structural response, providing a reliable tool for simulating the behaviour of partially grouted masonry walls under in-plane loading conditions.

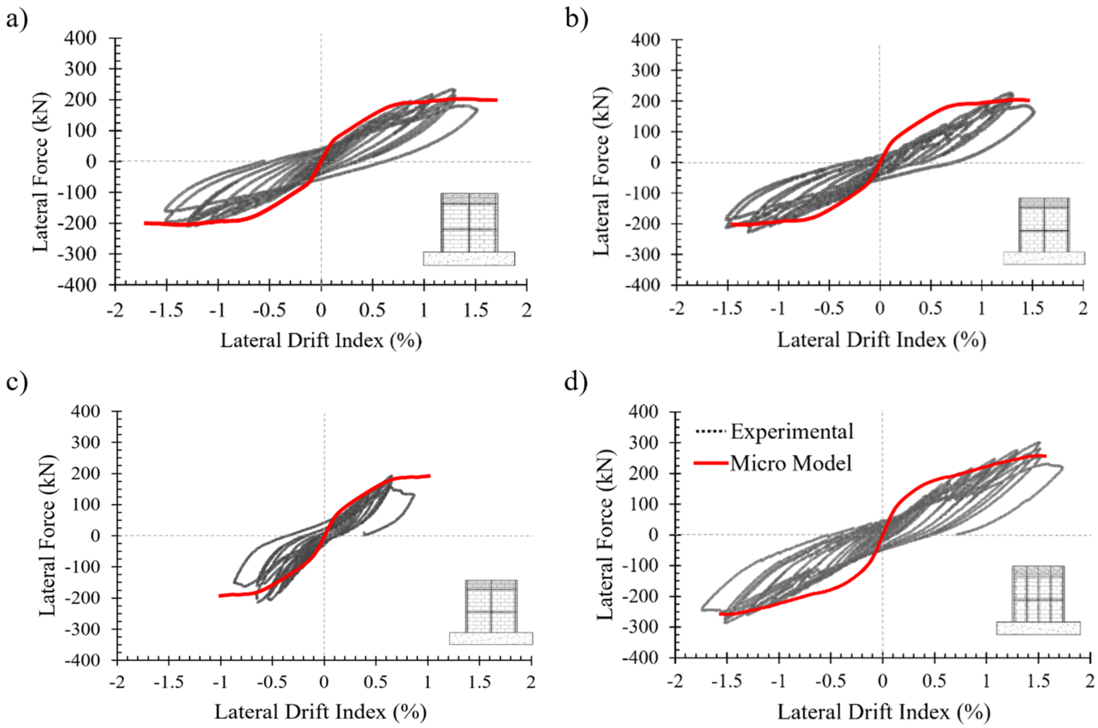

Figure 1: Applied Load – Wall Drift Comparison of FE Micro-Model and Tested Specimens (a) PG085-48 (b) PG120-48 (c) PG169-48 (d) PG085-24

Figure 6 illustrates the cyclic load–drift response of Specimen PG085-48. The micro-model demonstrated satisfactory performance in predicting the overall response, despite the absence of material damage models to account for cyclic degradation. This limitation is particularly evident when comparing the unloading behaviour of the experimental results with that of the micro-model. The experimental response exhibited significantly reduced stiffness during unloading cycles, which the micro-model failed to replicate due to the omission of cyclic degradation effects in the defined material interfaces and steel plasticity models.

The discrepancies observed emphasize the need for further investigation into the material properties and interface characteristics under cyclic loading. Additional experimental data would provide critical insights required to refine the micro-model and enable the incorporation of cyclic damage parameters. These enhancements would improve the model's ability to accurately simulate the cyclic behaviour of partially grouted masonry walls, ensuring a closer match to experimental observations and a more robust representation of structural performance under realistic loading conditions.

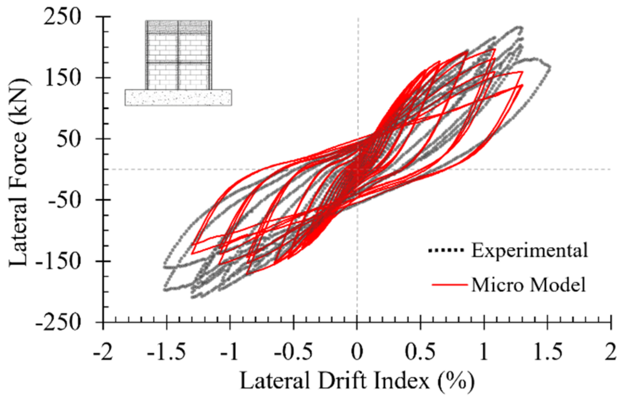

Figure 6: Cyclic Applied Load-Wall Drift Comparison for Specimen PG085-48

CONCLUSION

A detailed finite element micro-model was developed using the commercial software ABAQUS (Dassault Systems, 2022) to predict the in-plane shear capacity of partially grouted masonry walls, providing a foundation for enhancing the understanding of these wall systems. The model employed a two-layer representation, where the masonry unit flanges and mortar were grouped into one layer, and the masonry webs, grout, and steel reinforcement were grouped into another. These layers were coupled using a series of embedment constraints to simulate their interactions under loading conditions effectively.

To account for the material nonlinearity of masonry units, mortar, and grout, the Concrete Damage Plasticity (CDP) model, a plasticity-based material model, was implemented. The interaction between the masonry unit–mortar and masonry unit–grout interfaces was captured using a combination of a surface-based cohesion model and a Mohr-Coulomb friction law. This approach allowed the interface shear capacity to depend on the applied compressive loads, reflecting the behaviour observed in experimental triplet tests, which indicated that the mechanical response of the masonry unit–mortar interface aligns closely with the Mohr-Coulomb friction model.

The micro-model was validated by comparing its load–drift predictions with experimental results from full-scale masonry wall tests reported by Nolph and ElGawady. The validation included walls with varying aspect ratios, horizontal and vertical reinforcement quantities, and reinforcement distributions. The results demonstrated that the micro-model could accurately predict the ultimate load capacities, with deviations within 10% for the majority of the experimentally tested specimens. These findings underscore the micro-model's effectiveness in capturing the global and local behaviour of partially grouted masonry walls under in-plane shear loading.

DATA AVAILABILITY STATEMENT

Some or all data, models, or code that support the findings of this study are available from the corresponding author upon reasonable request.

REFERENCES

[1] Mayes, R., Omote, Y., and Clough, R. (1976a). "*Cyclic Shear Tests of Masonry Piers Volume 1 – Test Results.*" Report No. EERC-76-8, Earthquake Engineering Research Center, University of California Berkeley, USA.

[2] Mayes, R., Omote, Y., and Clough, R. (1976b). "*Cyclic Shear Tests of Masonry Piers Volume 2 – Analysis of Test Results.*" Report No. EERC-76-16, Earthquake Engineering Research Center, University of California Berkeley, USA.
[3] Chen, S., Hidalgo, P., Mayes, R., Clough, R., and McNiven, H. (1978). "*Cyclic Loading Tests of Single Masonry Piers – Volume 2: Height to Width Ratio of 1.*" Report No. UCB/EERC-78-28, Earthquake Engineering Research Center, University of California Berkeley, USA.
[4] Hidalgo, P., Mayes, R., McNiven, H., and Clough, R. (1979). "*Cyclic Loading Tests of Single Masonry Piers – Volume 3: Height to Width Ratio of 0.5.*" Report No. UCB/EERC-78-12, Earthquake Engineering Research Center, University of California Berkeley, USA.
[5] National Earthquake Hazards Reduction Program (NEHRP). (1994). "*NEHRP Recommended Provisions for Seismic Regulations for New Buildings – Part 1: Provisions.*" Building Seismic Safety Council, Washington, D.C.
[6] Canadian Standards Association (CSA). (2014). "*Design of Masonry Structures*." CSA S304-14 (R2019), CSA, Mississauga, Canada.
[7] Masonry Standards Joint Committee (MSJC). (2022). "Building Requirements and Specifications for Masonry Structures." TMS 402/602-22. Longmont, CO: Masonry Society.
[8] Hung, J. (2018). "*Artificial Neural Network Model for Analysis of In-Plane Shear Strength of Partially Grouted Masonry Shear Walls*." M.Sc. Thesis, University of Alberta, Alberta, Canada.
[9] Rahim, A., Pettit, C., Cruz-Noguez, C., and Hung, J. (2023a). "An Analysis Model for Partially Grouted Shear Walls Using Macro-Modelling: Importance of Reporting Joint Shear Strength." *Proc. Of the 14th North American Masonry Conference*. Omaha, USA.
[10] Elmeligy, O., Aly, N., & Galal, K. (2021). "Sensitivity analysis of the numerical simulations of partially grouted reinforced masonry shear walls." *Engineering Structures*, 245, 112876.
[11] Koutras, A. A., & Shing, P. B. (2020). "Seismic behavior of a partially grouted reinforced masonry structure: Shake-table testing and numerical analyses." *Earthquake Engineering & Structural Dynamics*, 49(11), 1115-1136.
[12] Al-Ahdal, A., Aly, N., & Galal, K. (2022). "Simplified analytical models for partially grouted reinforced masonry shear walls." *Engineering Structures*, 252, 113643.
[13] Calderón, S., Arnau, O., & Sandoval, C. (2019). "Detailed micro-modeling approach and solution strategy for laterally loaded reinforced masonry shear walls." *Engineering Structures*, 201, 109786.
[14] Calderón, S., Milani, G., & Sandoval, C. (2021). "Simplified micro-modeling of partially-grouted reinforced masonry shear walls with bed-joint reinforcement: Implementation and validation." *Engineering Structures*, 234, 111987.
[15] Dassault Systèmes. (2022). *ABAQUS 2022 User's Manual*. Dassault Systèmes Simulia Corp., Providence, RI, USA.
[16] Lubliner, J., Oliver, J., Oller, S., and Onate, E. (1989). "A Plastic-Damage Model for Concrete." *International Journal of Solids and Structures*, 25(3), 299–326.
[17] Lee, J., & Fenves, G. (1998). "Plastic-Damage Model for Cyclic Loading of Concrete Structures." *Journal of Engineering Mechanics*, 124(8), 892–899.
[18] Mohsin, E. (2005). "*Support Stiffness Effect on Tall Load Bearing Masonry Walls.*" Ph.D. Dissertation, University of Alberta, Alberta, Canada.
[19] Kmiecik, P., & Kaminski, M. (2011). "Modelling of Reinforced Concrete Structures and Composite Structures with Concrete Strength Degradation taken into Consideration." *Archives of Civil and Mechanical Engineering*, 11(3).
[20] Genikomsou, A., & Polak, M. (2014). "Finite Element Analysis of a Reinforced Concrete Slab-Column Connection using ABAQUS." Proc. *Structures Congress 2014*. Boston, USA.
[21] Michal, S., & Andrzej, W. (2015). "Calibration of the CDP Model Parameters in Abaqus." Proc. *2015 World Congress on Advances in Structural Engineering and Mechanics*. Incheon, Korea.
[22] Nasiri, E., & Liu, Y. (2017). "Development of a Detailed 3D FE Model for Analysis of the In-Plane Behaviour of Masonry Infilled Concrete Frames." *Engineering Structures*, 143, 603-616.

[23] Darmayadi, D., & Satyarna, I. (2019). "Finite Element Modeling of Masonry Wall with Mortar 1pc:4 Lime:10 Sand under Later Force." Proc. *MATEC Web of Conferences*, 258, 05019.

[24] Hognestad, E. (1951). "A Study of Combined Bending Axial Load in Reinforced Concrete Members." *Bulletin Series No. 399*, University of Illinois.

[25] Ross, M. (2013). "Recalibration of the Unit Strength Method for Determining the Compressive Strength of Grouted Concrete Masonry." M.Sc. Thesis, University of Alberta, Alberta, Canada.

[26] Priestley, M., & Elder, D. (1983). "Stress-Strain Curves for Unconfined and Confined Concrete Masonry." *ACI Structural Journal*, May-June, 192-201.

[27] Kent, D., & Park, R. (1971). "Flexural Members with Confined Concrete." *Journal of the Structural Division*, 97(7), 1969-1990.

[28] Vecchio, F., & Collins, M. (1986). "The Modified Compression-Field Theory for Reinforced Concrete Elements Subjected to Shear." *ACI Structural Journal*, 83(2), 219-231.

[29] Nayal, R., & Rasheed, H. (2006). "Tension Stiffening Model for Concrete Beams Reinforced with Steel and FRP Bars." *Journal of Materials in Civil Engineering*, 18(6), 831-841.

[30] Mazars, J. (1986). "A Description of Micro and Macroscale Damage of Concrete Structure." *Engineering Fracture Mechanics*, 25, 729–737.

[31] Mazars, J., Hamon, F. & Grange, S. (2015) "A new 3D damage model for concrete under monotonic, cyclic and dynamic loadings." *Materials and Structures*, 48, 3779–3793.

[32] Obaidat, A. (2017). "Compressive Behavior of C-Shaped Confined Masonry Boundary Elements." Ph.D. Dissertation, Concordia University, Québec, Canada.

[33] Birtel, V. and Mark, P. (2006). "Parameterized Finite Element Modelling of RC Beam Shear Failure." Proc. 2006 ABAQUS User's Conference.

[34] Nolph, S. and ElGawady, M. (2012). "Static Cyclic Response of Partially Grouted Masonry Shear Walls." Journal of Structural Engineering, 138(7), 864-879.

[35] Nolph, S. (2010). "In-Plane Shear Performance of Partially Grouted Masonry Shear Walls." M.Sc. Thesis, Washington State University, Washington, USA.

[36] Elmapruk, J. (2010). "Shear Strength of Partially Grouted Squat Masonry Shear Walls." M.Sc. Thesis, Washington State University, Washington, USA.